Electronic Supplementary Information

A Lead-Free Bismuth Iodide Organic-Inorganic Ferroelectric Semiconductor

Yu-Hua Liu,† Hang Peng† and Wei-Qiang Liao*

College of Chemistry, Nanchang University, Nanchang 330031, People's Republic of China

†These authors contributed equally to this work.

E-mail: liaowq@ncu.edu.cn

Experimental details

Materials. We synthesized [1,4-butanediammonium]I_2 first before the preparation of compound **1**. Stoichiometric amounts of hydriodic acid (57 wt. % in H_2O) were slowly added to the ethanol solution of 1,4-butanediamine under stirring. After removing the solvent by reduced pressure, solid sample of [1,4-butanediammonium]I_2 was obtained, which was then washed with diethyl ether and was dried in an oven. Compound **1** was synthesized by mixing equimolar amounts of [1,4-butanediammonium]I_2 and BiI_3 in hydriodic acid under stirring to get a clear solution. Dark-red crystals of **1** were obtained by slow evaporation of the solvent at 323 K. We confirmed the phase purity of as-grown crystals of **1** by powder X-ray diffraction (PXRD) analysis (Fig. S1).

Measurements. Single-crystal X-ray diffraction data were performed using Mo-Kα radiation (λ = 0.71073) on a Rigaku Saturn 924 diffractometer in the ω scan mode. The crystal data were collected at 293 K and 383 K, respectively. We used the CrystalClear software package to process the data. The crystal structures were solved by using the SHELXLTL software package. To record PXRD patterns, we used the

Rigaku D/MAX 2000 PC X-ray diffraction instrument in the 2θ between 5° and 50° with a step size of 0.02°. We used the NETZSCH DSC 200F3 instrument under a nitrogen atmosphere to record DSC curves. For SHG experiments, an unexpanded laser beam with low divergence (pulsed Nd:YAG at a wavelength of 1064 nm, 5 ns pulse duration, 1.6 MW peak power, 10 Hz repetition rate) was used. The instrument model is Ins 1210058, INSTEC Instruments, while the laser is Vibrant 355 II, OPOTEK. The dielectric measurements were performed on an automatic impedance Tonghui 2828 analyzer. We used the single-crystal plate with the thickness of 0.53 mm and the area of 1.8 mm^2 for the dielectric measurements. The large faces of the plate were painted with a silver conducting paste as the electrodes for dielectric studies. The *P-E* hysteresis loops were recorded on a Sawyer–Tower circuit, Precision Premier II (Radiant Technologies, Inc.). The PFM measurement was carried out on a commercial piezoresponse force microscope (Oxford instrument, Cypher ES) with high-voltage package and in-situ heating stage. PFM is based on the atomic force microscopy (AFM), with an AC drive voltage applied to the conductive tip. Conductive Ti/Ir-coated silicon probes (ASYELEC.01-R2, Oxford instrument) were used for domain imaging and polarization switching studies. UV-vis diffuse-reflectance spectra measurements were performed at room temperature using a Shimadzu UV-3600Plus spectrophotometer mounted with ISR-603 integrating sphere operating from 200 to 800 nm. $BaSO_4$ was used as a 100% reflectance reference. The generated reflectance-versus-wavelength data were used to estimate the band gap of the material by converting reflectance data to absorbance according to the Kubelka−Munk equation: $F(R_\infty) = (1- R_\infty)^2/2R_\infty$. Therefore, the optical band gap can be determined by the variant of the Tauc equation: $(h\nu \cdot F(R_\infty))^{1/n} = A(h\nu - E_g)$, Where: h: Planck's constant, ν: frequency of vibration, $F(R_\infty)$: Kubelka−Munk equation, E_g: band gap, A: proportional constant. The value of the exponent n denotes the nature of the sample transition. For direct allowed transition, n = 1/2; for indirect allowed transition, n = 2. Hence, the optical band gap E_g can be obtained from a Tauc plot by plotting $(h\nu \cdot F(R_\infty))^{1/n}$ against the energy in eV and extrapolation of the linear region to the X-axis intercept.

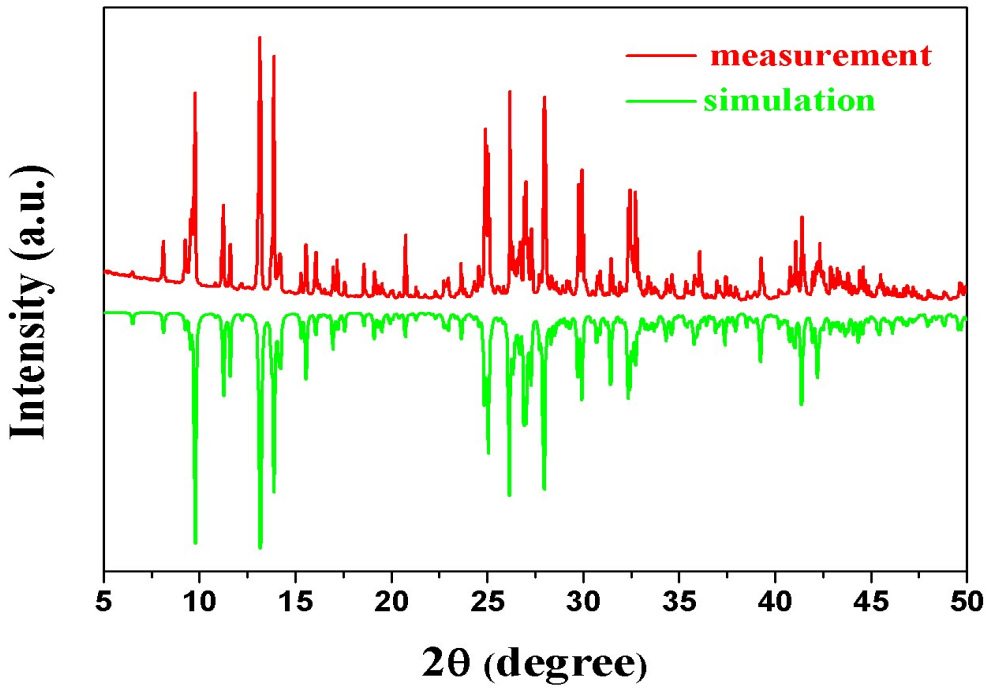

Figure S1. Experimental PXRD patterns of **1** at 293 K, matching with the simulated ones from crystal structure at 293 K.

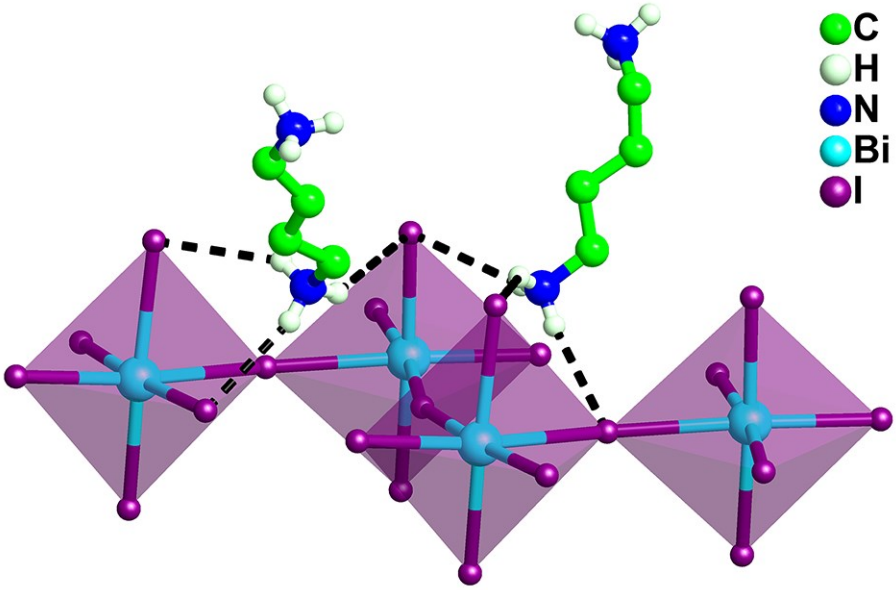

Figure S2. N–H···I hydrogen-bonding interactions (dash lines) between the $[BiI_5]_n^{2-}$ chains and the 1,4-butanediammonium cations.

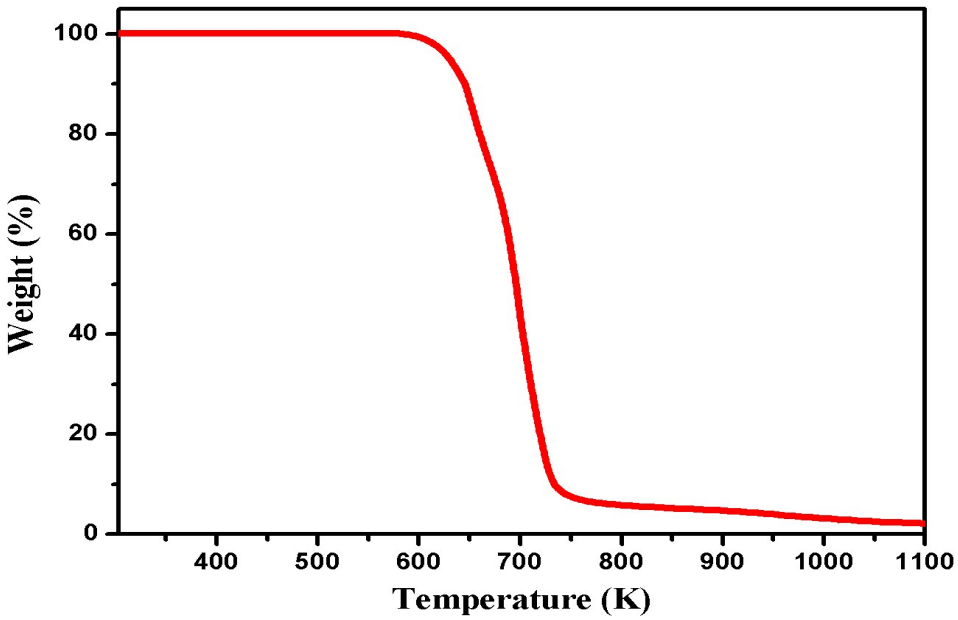

Figure S3. Thermogravimetric analysis (TGA) curve of **1**.

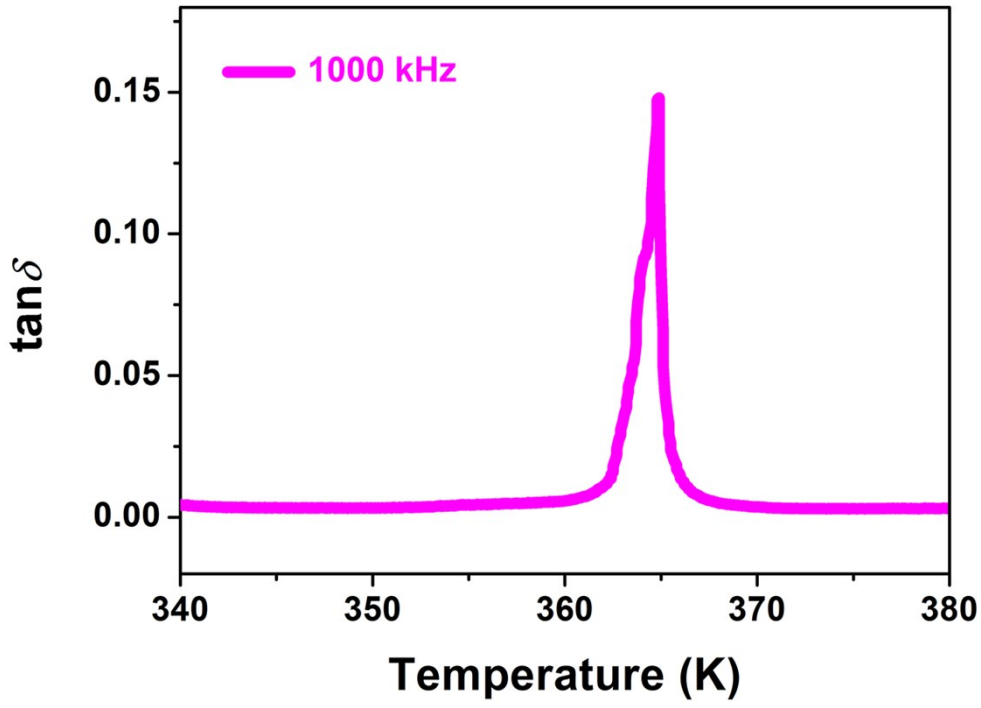

Figure S4. Temperature-dependent tanδ of the single-crystal sample of **1** along the polar *b* axis upon heating.

Table S1. Crystal data and structural refinements for **1** at 293 K and 383 K, respectively.

Moiety formula	$[NH_3(CH_2)_4NH_3]_3[BiI_5]_3$	
Temperature	293 K	383 K
Weight	2800.96	2800.96
Crystal system	Monoclinic	Monoclinic
Space group	$P2_1$	$P2_1/m$
a/Å	11.0339(9)	11.180(5)
b/Å	8.5608(4)	8.575(4)
c/Å	27.529(2)	27.548(13)
β/deg	99.793(5)	100.185(10)
Volume/Å^3	2562.4(3)	2599(2)
Z	2	2
$R1$ [$I>2\sigma(I)$]	0.0528	0.0725
$wR2$ [$I>2\sigma(I)$]	0.0875	0.1446
GOF	1.001	1.002

Table S2. Selected I−Bi bond lengths [Å] and I−Bi−I bond angles [°] for **1** at 293 K and 383 K.

Temperature	bond lengths [Å]		bond angles [°]			
293 K	Bi1—I1	2.9659 (12)	I1—Bi1—I2	88.48 (3)	I6—Bi2—I10	89.89 (3)
	Bi1—I2	3.1827 (10)	I1—Bi1—I3	90.10 (3)	I7—Bi2—I8	91.25 (3)
	Bi1—I3	3.2842 (11)	I1—Bi1—I4	100.20 (3)	I7—Bi2—I9	92.21 (3)
	Bi1—I4	2.9142 (12)	I1—Bi1—I5	92.56 (3)	I7—Bi2—I10	174.75 (3)
	Bi1—I5	3.0081 (10)	I1—Bi1—I6	173.11 (3)	I8—Bi2—I9	95.68 (3)
	Bi1—I6	3.2296 (11)	I2—Bi1—I3	86.82 (3)	I8—Bi2—I10	91.44 (3)
	Bi2—I3 ^{I}	3.2306 (12)	I2—Bi1—I4	89.93 (3)	I9—Bi2—I10	92.01 (3)
	Bi2—I6	3.2733 (11)	I2—Bi1—I5	176.62 (3)	I11—Bi3—I12	89.85 (3)
	Bi2—I7	3.0392 (10)	I2—Bi1—I6	90.59 (3)	I11—Bi3—I13	86.69 (3)

	Bi2—I8	2.9524 (11)	I3—Bi1—I4	169.12 (4)	I11—Bi3—I13^{II}	90.30 (3)
	Bi2—I9	2.9210 (11)	I3—Bi1—I5	89.95 (3)	I11—Bi3—I14	175.67 (3)
	Bi2—I10	3.1231 (10)	I3—Bi1—I6	83.04 (3)	I11—Bi3—I15	89.50 (3)
	Bi3—I11	3.1778 (10)	I4—Bi1—I5	93.06 (3)	I12—Bi3—I13	91.14 (4)
	Bi3—I12	2.9277 (12)	I4—Bi1—I6	86.62 (3)	I12—Bi3—I13^{II}	91.14 (4)
	Bi3—I13	3.2585 (15)	I5—Bi1—I6	87.99 (3)	I12—Bi3—I14	93.74 (3)
	Bi3—I13^{II}	3.2556 (15)	I3^{I}—Bi2—I6	84.29 (3)	I12—Bi3—I15	95.92 (3)
	Bi3—I14	2.9933 (10)	I3^{I}—Bi2—I7	90.04 (3)	I13—Bi3—I13^{II}	82.260 (12)
	Bi3—I15	2.9475 (12)	I3^{I}—Bi2—I8	176.81 (3)	I13—Bi3—I14	89.46 (3)
			I3^{I}—Bi2—I9	87.18 (3)	I13—Bi3—I15	90.68 (4)
			I3^{I}—Bi2—I10	87.05 (3)	I13^{II}—Bi3—I14	87.22 (3)
			I6—Bi2—I7	85.47 (3)	I13^{II}—Bi3—I15	172.94 (4)
			I6—Bi2—I8	92.90 (3)	I14—Bi3—I15	92.53 (3)
			I6—Bi2—I9	171.16 (3)		
383 K	Bi1—I1	3.170 (2)	I1—Bi1—I2	88.71 (4)	I6—Bi2—I8^{V}	177.92 (6)
	Bi1—I2	3.2710 (11)	I1—Bi1—I2^{III}	88.71 (4)	I6^{V}—Bi2—I7	91.69 (4)
	Bi1—I2^{III}	3.2710 (11)	I1—Bi1—I3	175.96 (5)	I6^{V}—Bi2—I8	169.32 (6)
	Bi1—I3	3.0007 (19)	I1—Bi1—I4	89.22 (4)	I6^{V}—Bi2—I8^{V}	85.75 (6)
	Bi1—I4	2.9395 (14)	I1—Bi1—I4^{IV}	89.22 (4)	I7—Bi2—I8	85.19 (6)
	Bi1—I4^{IV}	2.9395 (14)	I2—Bi1—I2^{III}	81.90 (4)	I7—Bi2—I8^{V}	89.57 (6)
	Bi2—I5	3.030 (2)	I2—Bi1—I3	88.24 (4)	I8—Bi2—I8^{V}	84.02 (7)
	Bi2—I6	2.9337 (15)	I2—Bi1—I4	91.53 (4)	I8—Bi3—I8^{VI}	81.79 (7)
	Bi2—I6^{V}	2.9337 (15)	I2—Bi1—I4^{IV}	173.15 (3)	I8—Bi3—I9	85.99 (6)
	Bi2—I7	3.118 (2)	I2^{III}—Bi1—I3	88.24 (4)	I8—Bi3—I10	84.90 (6)
	Bi2—I8	3.216 (3)	I2^{III}—Bi1—I4	173.15 (3)	I8—Bi3—I10^{VI}	174.57 (6)
	Bi2—I8^{V}	3.282 (3)	I2^{III}—Bi1—I4^{IV}	91.53 (4)	I8—Bi3—I11	91.58 (6)

Bi3—I8	3.295 (3)	I3—Bi1—I4	93.51 (4)	I8^{VI}—Bi3—I9	90.59 (6)
Bi3—I8^{VI}	3.206 (3)	I3—Bi1—I4^{IV}	93.51 (4)	I8^{VI}—Bi3—I10	166.14 (6)
Bi3—I9	3.010 (2)	I4—Bi1—I4^{IV}	94.98 (6)	I8^{VI}—Bi3—I10^{VI}	93.08 (6)
Bi3—I10	2.9381 (15)	I5—Bi2—I6	92.36 (4)	I8^{VI}—Bi3—I11	86.66 (7)
Bi3—I10^{VI}	2.9381 (15)	I5—Bi2—I6^{V}	92.36 (4)	I9—Bi3—I10	92.32 (4)
Bi3—I11	3.155 (2)	I5—Bi2—I7	173.96 (6)	I9—Bi3—I10^{VI}	92.32 (4)
		I5—Bi2—I8	90.02 (6)	I9—Bi3—I11	176.57 (5)
		I5—Bi2—I8^{V}	86.26 (6)	I10—Bi3—I10^{VI}	100.33 (6)
		I6—Bi2—I6^{V}	95.87 (6)	I10—Bi3—I11	89.87 (4)
		I6—Bi2—I7	91.68 (4)	I10^{VI}—Bi3—I11	89.88 (4)
		I6—Bi2—I8	94.43 (6)		

Symmetry code(s): (Ⅰ) x, -1+y, z; (Ⅱ) 2-x, 1/2+y, 1-z; (Ⅲ) 2- x, -1/2+y, 1-z; (Ⅳ) x, 1/2-y, z; (Ⅴ) x, 3/2-y, z; (Ⅵ) x, 5/2-y, z.